PHYSICAL REVIEW B

CONDENSED MATTER

THIRD SERIES, VOLUME 48, NUMBER 5 1 AUGUST 1993-I

Effect of the form of the height-height correlation function on diffuse x-ray scattering from a self-affine surface

G. Palasantzas and J. Krim

Physics Department, Northeastern University, Boston, Massachusetts 02115

(Received 22 January 1993)

Height-height correlations for self-affine surfaces with finite horizontal cutoffs are generally modeled by exponential forms. Three mathematically acceptable, alternate forms for the height-height correlation function are investigated, to explore their impact on the analysis of diffuse x-ray-reflectivity data. The appropriateness of these functions to actual physical samples is explored through comparison with x-ray-reflectivity and scanning-tunneling-microscopy data recorded on known self-affine surfaces.

I. INTRODUCTION

A wide variety of surfaces and interfaces occurring in nature are well represented by a kind of roughness associated with self-affine fractal scaling, defined by Mandelbrot in terms of fractional Brownian motion.[1] Examples include the nanometer scale topology of vapor-deposited films,[2] the spacial fluctuations of liquid-gas interfaces,[3] and the kilometer-scale structures of mountain terrain.[1] Physical processes which produce such surfaces include fracture, erosion, and molecular beam epitaxy, as well as fluid invasion of porous media.[4] All rough surfaces exhibit perpendicular fluctuations, which are characterized by a mean-square roughness $\sigma=\langle z(x,y)^2\rangle^{1/2}$, $z(x,y)=h(x,y)-\langle h(x,y)\rangle$, where $h(x,y)$ is the height function and $\langle\cdots\rangle$ is the spacial average over a planar reference surface. The roughness is termed "Gaussian" if $z(x,y)-z(x',y')$ is a Gaussian random variable whose distribution depends only on the relative coordinates $(X,Y)\equiv(x'-x,y'-y)$. For an isotropic Gaussian rough surface, the mean-square surface fluctuation $g(R)$ is written as

$$g(R)=\langle[z(x',y')-z(x,y)]^2\rangle ,$$
$$R=\sqrt{(X^2+Y^2)} ,$$

where the average is taken over all pairs of points on the surface which are separated horizontally by the length R. The function $g(R)$ is related to the height-height correlation function $C(R)=\langle z(R)z(0)\rangle$ by

$$g(R)=2\langle z(x,y)^2\rangle-2\langle z(x,y)z(x',y')\rangle$$
$$=2\sigma^2-2\langle z(R)z(0)\rangle . \quad (1)$$

If the surface exhibits self-affine roughness, $g(R)$ will scale as $g(R)\propto R^{2H}$,[5] where $0<H<1$ is referred to as the "roughness" exponent.[6]

The mean-square roughness of any physical self-affine surface will saturate at sufficiently large horizontal lengths. It is thus characterized by a correlation length ξ, such that

$$R\ll\xi,\quad g(R)\propto R^{2H} , \quad (2a)$$
$$R\gg\xi,\quad g(R)=2\sigma^2 . \quad (2b)$$

Diffuse x-ray-reflectivity measurements, sensitive to surface height-height correlations, can be employed to experimentally probe the parameters ξ and H.[7,8] Investigators generally use the correlation function suggested by Sinha *et al.*,[7]

$$C_S(R)=\sigma^2 e^{-(R/\xi)^{2H}} , \quad (3)$$

to fit diffuse reflectivity data.[2,9,10] Several reasons justify this choice. Equation (3) is mathematically convenient, and also allows for correct scaling of $g(R)$ in the Eqs. (2) limits. Exponential forms for correlation functions are well founded in equilibrium critical phenomena, where the asymptotic, noncritical behavior of the total pair correlation function of a fluid,[11] $C(R)\sim R^{-1}e^{-aR}$, as well as that of simple Brownian motion considered as an Ornstein-Uhlenbeck process, $C(R)\sim e^{-aR}$,[12] are treated as such. Numerous self-affine surfaces are formed, however, under *nonequilibrium* conditions.[13] This, along with the fact that experimentally relevant length scales require that $C(R)$ be correct for $R\sim\xi$ [as well as in the Eqs. (2) limits], suggest that further examination of the form of $C(R)$ is in order.

We propose here three mathematically acceptable, alternate forms for $C(R)$ (Sec. II), and examine their impact on the analysis of diffuse reflectivity data (Sec. III). Through comparison with diffuse reflectivity and scanning tunneling microscopy (STM) data for known self-

affine surfaces (cold-deposited Ag), we examine the extent to which these functions might provide a better description of the height-height correlations for actual samples (Sec. IV). Our efforts reveal that the original exponential form for $C(R)$ remains as the most satisfactory form, for the samples that we have examined.

II. ALTERNATE CORRELATION FUNCTIONS

We propose the following three alternate forms for the height-height correlation function:

$$C_{PK1}(R)=\sigma^2(1-\tanh^{2H}(R/\xi)) , \tag{4}$$

$$C_{PK2}(R)=\sigma^2(1-e^{-(R/\xi)H}[2\cosh(R/\xi)-2]^H) , \tag{5}$$

$$C_{PK3}(R)=\sigma^2(1-[1-e^{-(R/\xi)^2}]^H) . \tag{6}$$

These functions are put forward solely on account of their mathematical correctness in terms of the Eqs. (2) limits, and not on any specific physical grounds. Nonetheless, it is enlightening to examine the impact of these alternate forms on the analysis of x-ray-reflectivity data. Figure 1 depicts each of the functions, as well as C_S, in the range $0<R<3\xi$ for two different values of H (0.3 and 0.7). As the value of H decreases, all four functions exhibit increased decay rates for $R<\xi$. This is especially pronounced for C_{PK2} (dot-dashed line), whose decay rate exceeds that of C_S (solid line) for the lower values of H. The rate of decrease is relatively steady for C_{PK1} (long-dashed line) and C_{PK3} (short-dashed line), but slows substantially after $R\sim\xi$ for C_{PK2} and C_S. We note that the primary differences between the functions exist at $R\sim\xi$. For $R\ll\xi$, and $R\gg\xi$, the functions are virtually identical.

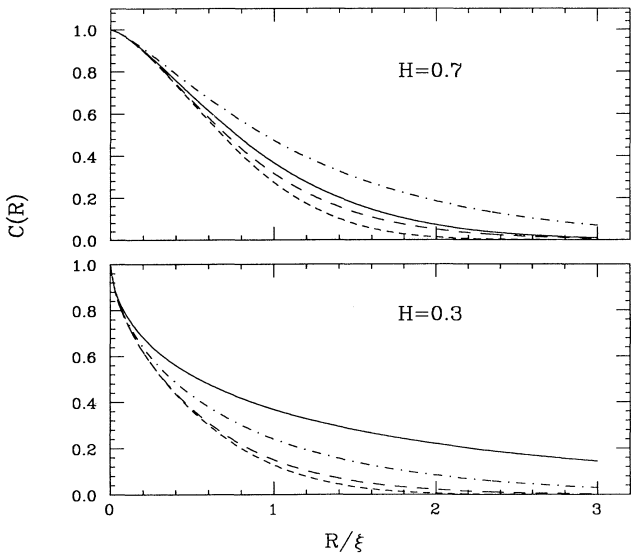

FIG. 1. Height-height correlation functions for $\sigma=1.0$ and two values of H (0.3 and 0.7). Solid lines: C_S, long-dashed lines: C_{PK1}, dot-dashed lines: C_{PK2}, and short-dashed lines C_{PK3}.

III. DIFFUSE X-RAY REFLECTIVITY

A. Theory of the diffuse scattering from a self-affine surface

Specular (angle of incidence θ equal to angle of reflection) reflection of x rays from surfaces yields information about the mean-square roughness and also the sample's electron density distribution.[7,14] Such measurements involve recording the scattered intensity as a function of $q_z=(4\pi/\lambda)\sin(\theta)$, where q_z is the wave-vector transfer perpendicular to the surface. The diffuse (angle of incidence not equal to the angle of reflection) component of the scattering is related to height-height correlations of the rough surface. Sinha *et al.*[7] used perturbation theory on the exact solution of the wave equation for a smooth surface to calculate the diffuse scattering produced by surface roughness [Eqs. (4.41) and (4.42) in their paper]. Experimental data are normally recorded with the parallel detector slit (in the plane of the surface, and out of the scattering plane) wide open.[2,9,10] The Ref. 7 expressions for diffuse scattering, integrated with respect to this y direction, are then given as

$$I(q_x)=I_0\frac{\Delta\Omega}{A}(L_xL_y)\frac{|k_0^2(1-n)^2|^2}{16\pi^2}\times|T(\mathbf{k}_1)|^2|T(\mathbf{k}_2)|^2S(q_x) , \tag{7a}$$

$$S(q_x)=\frac{\exp\{-[(q_z^t)^2+(q_z^{t*})^2]\sigma^2/2\}}{|q_z^t|^2}\times\int_0^\infty(e^{|q_z^t|^2C(X)}-1)\cos(q_xX)dX , \tag{7b}$$

where $\mathbf{k}_1$ ($\mathbf{k}_2$), are the incident (reflected) wave vectors, k_0 the wave vector magnitude, q_x and q_z^t the in-plane x-component and in-medium z component of the wave-vector transfer, $T(\mathbf{k})$ the Fresnel transmission coefficient, n the index of refraction, L_xL_y the area illuminated by the beam, I_0 and A the intensity and cross-sectional area of the beam, and $\Delta\Omega$ the solid angle subtended by the detector at the sample.

The diffuse cross-section (recorded at specular condition) of a self-affine surface with no cutoff [Eq. (7) with $\xi=\infty$ and $q_x=0$] has the form[15]

$$I(q_z)\propto(L_xL_y)q_z^{-[2+(1/H)]} . \tag{8}$$

A plot of the diffuse intensity at specular condition versus q_z can therefore in principle provide an experimental determination of the parameter H. Since there are both specular and diffuse contributions to the scattering intensity recorded at specular condition, the sample is offset slightly from the specular condition to remove the specular component. If the incident angle is θ_1, then the intensity is measured at an angle $\theta_2=\theta_1\pm\epsilon$ where $\epsilon\ll\theta_1$, but large enough to eliminate the specular contribution.

The parameter ξ is determined by examining the diffuse scattering component of a Yoneda, or rocking curve scan. In this geometry, the detector is held at a fixed angle, and the sample is rocked about the specular condition. A central maximum in the intensity I_s for

such a scan corresponds to the specular condition $\theta_1=\theta_2$. The scattering profile also has intensity peaks I_w at the critical angle θ_c for total external reflection $\theta_1,\theta_2=\theta_c$. The diffuse region outside of the central maximum can be fit to Eq. (7) to yield an experimental value for the correlation length.

B. Selected numerical results

As discussed above, the slope of an "off-specular" reflectivity curve under ideal conditions ($\xi=\infty$, $q_x=0$), is $2+(1/H)$. In practice, however, the correlation length ξ is finite and the experimental data are not recorded at precisely $q_x=0$. Theoretical off-specular curves for a typical set of experimental parameters [$\xi=4000$ Å, $\epsilon=0.03°(q_x\sim10^{-4}$ Å$^{-1})$, $H=0.3$, $\sigma=7$ Å, $\lambda=1.5337$ Å, and $n=1-6.3\times10^{-6}-i8.5\times10^{-8}$] are depicted in Fig. 2 for the functions C_S and C_{PK1}. In spite of the finite values for ξ and q_x, each curve tends towards a linear regime with slope $-[2+(1/H)]$ at sufficiently large q_z.

The inset to Fig. 2 depicts the value of H obtained from a fit to the slope of off-specular data, versus the actual value of H, for C_{PK1} (circles) and C_S (stars). The function C_S yields a consistently low value for H, with the discrepancy ranging from 0.02 for low H, to 0.04 for the higher values. The corresponding discrepancy for C_{PK1} is ~0 to 0.02. The Fig. 2 data are representative of a wide range of parameters which have been examined for all four functions. In general, we observe that linear fits to data recorded above $q_z\sigma=1$ yields values for H, which are lower than, but within 0.05 of the true value of H.

Figure 3 depicts selected Yoneda curves generated with the same parameters as above, except that ξ and σ are, respectively, varied from 700–7000 Å (left side), and 7–36 Å (right-hand side), for both C_S (solid lines) and C_{PK1} (dashed lines). The two correlation functions yield curves which are distinctly different in form. The value for ξ obtained from a fit to a Yoneda curve clearly depends on the assumed form of the correlation function. The extent of these differences is highlighted in Fig. 4, which depicts the quantity $d_s-d_w=\ln(I_s)-\ln(I_w)$ for

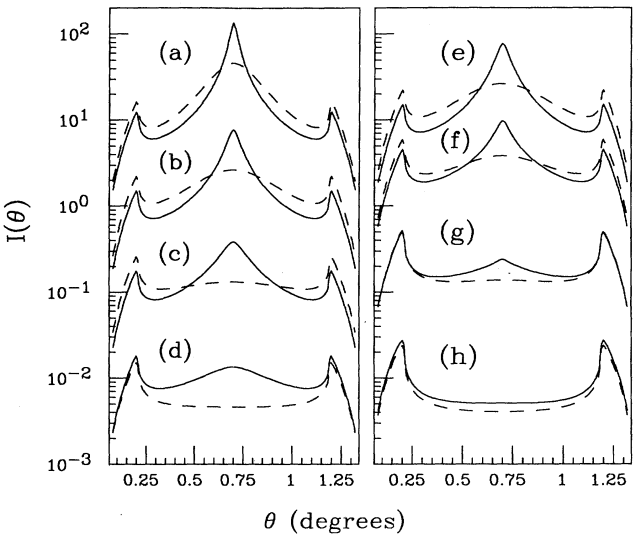

FIG. 3. Yoneda curves for C_S (solid lines) and C_{PK1} (dashed lines) for $H=0.3$. Left side: $\sigma=7.0$ Å and $\xi=$ (a) 700, (b) 2000, (c) 4000, (d) 7000 Å. Right side: $\xi=4000$ Å and $\sigma=$(e) 7, (f) 15, (g) 25, (h) 36 Å. The scaling factors are, respectively, 10^0 (a) and (e), 10^{-1} (b) and (f), 10^{-2} (c) and (g), and 10^{-3} (d) and (h).

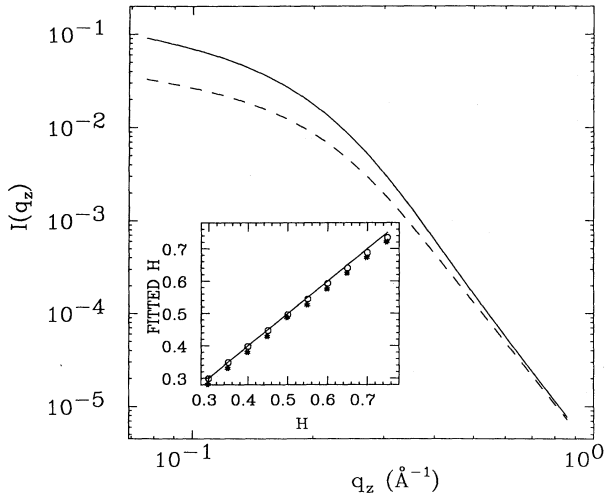

FIG. 2. Off specular reflectivity curves for $H=0.3$, $\xi=4000.0$ Å, $\sigma=7.0$ Å, and $\epsilon=0.03°$. Solid line: C_S and dashed line: C_{PK1}. The inset shows the value of H determined from the slope according to Eq. (8) vs the actual value of H, for C_S (stars) and C_{PK1} (circles). The solid line in the inset corresponds to $H_{\rm fit}=H$.

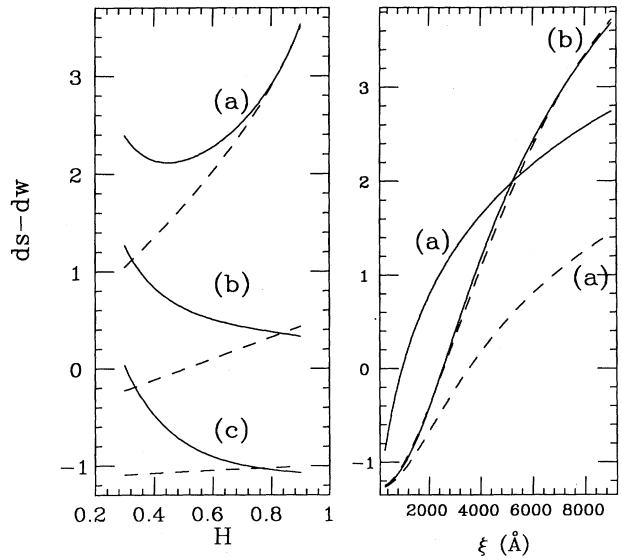

FIG. 4. Plots of d_s-d_w for C_S (solid lines), and C_{PK1} (dashed lines). Left side: $\sigma=7$ Å and $\xi=$ (a) 7000, (b) 3000, and (c) 1000 Å. Right side: $\sigma=7$ Å, and (a) $H=0.3$ and (b) $H=0.7$.

both C_S and C_{PK1} and a variety of parameters. The differences in the curves result directly from differences in the decay rates for $R<\xi$ and $R>\xi$, as H varies. It is evident that a physically appropriate form for the correlation function is essential if a meaningful value for ξ is to be obtained.

IV. COMPARISON WITH EXPERIMENT

We have thus far argued that the form of the correlation function near $R\sim\xi$ is indeed important to the analysis of diffuse x-ray data, in particular when the analysis involves a Yoneda scan. However, we have provided no compelling physical justification to select a particular function. We next examine the physical appropriateness of the various functions through direct comparison with x-ray reflectivity and STM data, recorded on known self-affine surfaces.

We first consider the Yoneda data reported by Chiarello *et al.*[2] recorded on a 1100-Å-thick Ag film, which was thermally evaporated onto polished quartz held at 80 K. Fits employing C_S yielded $H=0.46$ and $\xi=1450$ Å for this sample. Figure 5 shows the Ref. 2 Yoneda data, along with curves generated for the four functions considered here, each employing the same values of H and ξ. To facilitate the comparison, experimental data are shown on both the left and right sides of the figure. Inspection of Fig. 5 reveals C_S and C_{PK2} to be the best matches for the overall shape of the experimental data. In particular, we note that the region between the central maximum and the outer "wing" area is concave upward in the experimental curve. This feature is not present for the C_{PK1} and C_{PK3} curves, unless the value of ξ is increased to physically unrealistic values.

Fits to the Yoneda data described above are dominated by horizontal lengths exceeding 60 nm (Fig. 5, upper scale). In order to focus on a somewhat shorter horizontal length scale, as well as to explore an alternate experimental approach, we examined STM data recorded on a second cold-deposited silver film sample. The sample was prepared by thermal evaporation of 1000 Å of Ag onto polished quartz held at 106 K. Four 500×500 $(\text{nm})^2$ images were recorded in a dry N_2 environment with a commercial (Digital Instruments Nanoscope II) STM, with a grid density of 400 lines by 400 points per line. Height-height correlations were computed directly from the four data sets, averaged, and then fit to the various functions considered in this work (Fig. 6).

The best fit to the data by the C_S function yielded the values $H=0.64$ (Fig. 6, inset) and $\xi=13.0$ nm. The value of ξ compared favorably with characteristic cluster sizes observed in the STM images. We note the discrepancy between H and ξ for this sample and those of Ref. 2 sample, potentially due to differences in the two samples' preparation conditions. Further studies on samples prepared under identical conditions[10] will be necessary to resolve this issue. For the present work, we focus on the appropriateness of the functional form used to model actual height-height correlations.

Examination of four curves in Fig. 6 reveals C_{PK2} to be the best fit to the data for the entire range of lengths probed, and C_S to be the best fit for the range $R<2\xi$. Once more, the functions C_{PK1} and C_{PK3} are less descriptive of the actual experimental data. We conclude that for $R\leq\xi$, actual height-height correlations are in fact quite adequately described by the original exponential form which has been assumed in previous investigations. At large length scales, the height-height correlations appear to be tending more towards a form $R^a e^{-R}$, suggest-

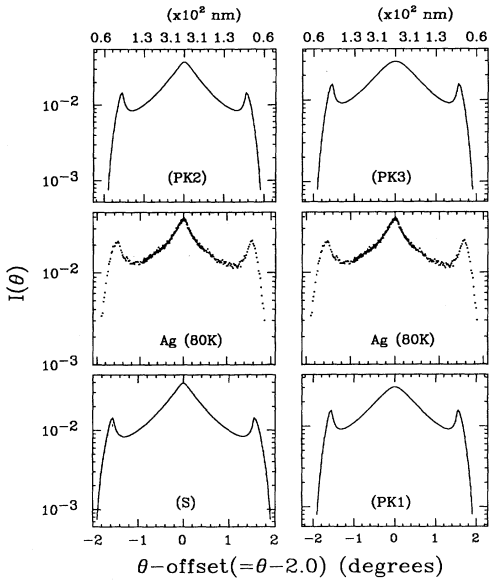

FIG. 5. Comparison of Ref. 2 Yoneda data to theoretically generated curves for the four functions considered here, employing $H=0.46$, $\xi=1450$ Å, $\sigma=8.5$ Å. The upper scale depicts the characteristic horizontal lengths $\approx 2\pi/q_x$ probed in this scan, which range from about 60 to 600 nm.

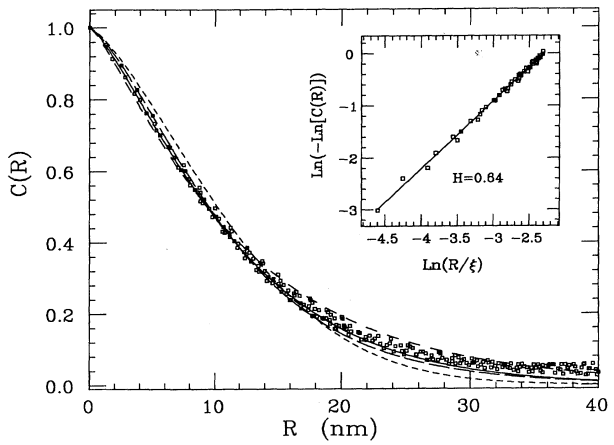

FIG. 6. Plots of the best fits of the four functions considered here to correlation data obtained from scanning tunneling microscopy (squares). C_S (solid line), $\xi=13$ nm; C_{PK1} (long-dashed line), $\xi=15.2$ nm; C_{PK2} (medium-dashed line), $\xi=16.2$ nm, C_{PK3} (short-dashed line), $\xi=11.0$ nm. The inset shows the linear fit to determine $H=0.64\pm0.02$ according to C_S.

ed by the decreased decay rate of the data in the range $2\xi < R < 4\xi$.

VI. CONCLUSIONS

We have presented here three mathematically acceptable, alternate forms for the height-height correlation function of a self-affine surface with a finite horizontal cutoff. We have explored their impact on diffuse x-ray reflectivity data, and found only a slight effect on the parameter H, which is obtained from a fit to Eq. (8). This can be understood in terms of the relatively short lengths which are sampled to determine H. Well below the horizontal cutoff ξ, all four functions scale in a similar manner.

Not surprisingly, the value of ξ obtained from fits to the x-ray Yoneda scans is highly sensitive to the form of the correlation function which has been assumed. Our comparisons with diffuse x-ray reflectivity and STM data reveal two of the functions, C_S and C_{PK2} as satisfactory in form. The function C_{PK2} exhibits exponential decay for $R \gg \xi$, where $C_{PK2}(R) \sim 2H\sigma^2 e^{-HR/\xi}$. The function, C_S is the exponential form which is in common use. We consider it the preferable function on account of its mathematical simplicity, and the fact that for $H = 0.5$, it reduces to the simple physical case of Brownian motion.

ACKNOWLEDGMENTS

We wish to thank P. Pfeifer and S. K. Sinha for useful discussions. This work was supported by NSF Grant No. DMR9204022.

[1]B. B. Mandelbrot, *The Fractal Geometry of Nature* (Freeman, New York, 1982).

[2]R. Chiarello, V. Panella, J. Krim, and C. Thompson, Phys. Rev. Lett. **67**, 3408 (1991).

[3]J. H. Sikkenk, J. M. J. van Leeuwen, E. O. Vossnack, and A. F. Bakker, Physica A **146**, 622 (1987).

[4]M. W. Mitchell and D. A. Bonnell, J. Mater. Res. **5**, 2244 (1990); E. A. Eklund *et al.*, Phys. Rev. Lett. **67**, 1759 (1991); J. Krim *et al.*, *ibid.* **70**, 57 (1993); D. A. Kessler *et al.*, *ibid.* **69**, 100 (1992); M. A. Rubio *et al.*, *ibid.* **63**, 1685 (1989); V. K. Horvath *et al.* J. Phys. A **24**, L25 (1991).

[5]For a review, see F. Family and T. Vicsek, *Dynamics of Fractal Surfaces* (World Scientific, Singapore, 1991).

[6]J. Krim and J. O. Indekeu, Phys. Rev. E (to be published).

[7]S. K. Sinha, E. B. Sirota, S. Garoff, and H. B. Stanley, Phys. Rev. B **38**, 2297 (1988).

[8]P.-Z. Wong and A. J. Bray, Phys. Rev. B **37**, 7751 (1988).

[9]D. E. Savage *et al.*, J. Appl. Phys. **69**, 1411 (1991).

[10]W. Weber and B. Lengler, Phys. Rev. B **46**, 7953 (1992).

[11]H. E. Stanley, *Introduction to Phase Transitions and Critical Phenomena* (Oxford University Press, New York, 1971), pp. 94–108.

[12]D. T. Gillespie, *Markov Processes: An Introduction for Physical Scientists* (Academic, Boston, 1992), p. 159.

[13]T. Vicsek, *Fractal Growth Phenomena* (World Scientific, Singapore, 1989).

[14]A. Braslau, P. S. Pershan, G. Swislow, and B. M. Ocko, Phys. Rev. A **38**, 2457 (1988).

[15]This relation was pointed out to us by S. K. Sinha, who also noted that $(L_x L_y)$ is in general dependent on q_z.